Hepatic Steatosis and Ectopic Fat Are Associated With Differences in Subcutaneous Adipose Tissue Gene Expression in People With HIV

Curtis L. Gabriel,[1,2] Fei Ye,[3] Run Fan,[3] Sangeeta Nair,[4] James G. Terry,[4] John Jeffrey Carr,[4] Heidi Silver,[1,5] Paxton Baker,[6] LaToya Hannah,[7] Celestine Wanjalla,[2,8] Mona Mashayekhi,[7] Sam Bailin,[8] Morgan Lima,[2] Beverly Woodward,[2] Manhal Izzy (ID) ,[1] Jane F. Ferguson,[9] and John R. Koethe[2,5,8]

Persons with human immunodeficiency virus (PWH) have subcutaneous adipose tissue (SAT) dysfunction related to antiretroviral therapy and direct viral effects, which may contribute to a higher risk of nonalcoholic fatty liver disease compared with human immunodeficiency virus–negative individuals. We assessed relationships between SAT expression of major adipocyte regulatory and lipid storage genes with hepatic and other ectopic lipid deposits in PWH. We enrolled 97 PWH on long-term antiretroviral therapy with suppressed plasma viremia and performed computed tomography measurements of liver attenuation, a measure of hepatic steatosis, skeletal muscle (SM) attenuation, and the volume of abdominal subcutaneous, visceral, and pericardial adipose tissue. Whole SAT gene expression was measured using the Nanostring platform, and relationships with computed tomography imaging and fasting lipids were assessed using multivariable linear regression and network mapping. The cohort had a mean age of 47 years, body mass index of 33.4 kg/m^{2}, and CD4 count of 492 cells/mm^{3}. Lower liver attenuation, a marker of greater steatosis, was associated with differences in SAT gene expression, including lower lipoprotein lipase and acyl-CoA dehydrogenase, and higher phospholipid transfer protein. Lower liver attenuation clustered with lower visceral adipose tissue (VAT) attenuation and greater VAT volume, pericardial fat volume and triglycerides, but no relationship was observed between liver attenuation and SAT volume, SM attenuation, or low-density lipoprotein. *Conclusion:* Liver attenuation was associated with altered SAT expression of genes regulating lipid metabolism and storage, suggesting that SAT dysfunction may contribute to nonalcoholic fatty liver disease in PWH. SAT gene-expression relationships were similar for VAT volume and attenuation, but not SM, indicating that ectopic lipid deposition may involve multiple pathways. (*Hepatology Communications* 2021;5:1224-1237).

L iver disease has emerged as the second most common cause of death in persons with human immunodeficiency virus (HIV) (PWH) in the United States.[(1)] The development of nonalcoholic fatty liver disease (NAFLD) and its sequelae comprise a significant share of liver-related morbidity

View this article online at wileyonlinelibrary.com.

and mortality among PWH. The rising burden of NAFLD is part of a growing increase in cardiometabolic diseases, including hypertension, hyperlipidemia, and type 2 diabetes in an aging HIV population that is also becoming more overweight and obese.[2-6] The global prevalence of NAFLD was estimated at 25% in 2016,[7] whereas the global prevalence of NAFLD among PWH specifically was estimated at 35% in a 2017 meta-analysis.[4] NAFLD occurs at a lower body mass index (BMI) and in the setting of greater physical activity in PWH compared with HIV-negative persons,[8] and PWH with NAFLD develop steatohepatitis and hepatic fibrosis at higher rates.[5,6]

The increased prevalence of NAFLD among PWH is multifactorial, but impaired subcutaneous adipose tissue (SAT) lipid storage may contribute to the accumulation of ectopic lipid deposits in liver, visceral adipose tissue (VAT), the heart and skeletal muscle (SM), and other organs. SAT constitutes the body's primary lipid storage depot, and research in the obesity field has demonstrated the malleability of SAT and the consequences of disrupted adipocyte cellular regulation and energy storage for metabolic health.[9] Both HIV *per se* and antiretroviral medications can affect adipose tissue quantity, distribution, and contribution to metabolic homeostasis through effects on adipocytes and stromal vascular cells.[10,11] Fibrosis and inflammation in the SAT of PWH impair normal energy storage and promote a state of excess circulating lipids that accumulate in other compartments that are less susceptible to HIV-related dysregulation, such as VAT.[12]

Computed tomography (CT) imaging is a noninvasive tool to estimate ectopic lipid deposition in the liver and SM, and to assess the volume and structure of adipose tissue depots. CT radiation attenuation—measured in Hounsfield units (HU)—is used to characterize the density of these compartments. Lower liver and SM attenuation correlates with higher tissue lipid content, and an attenuation of 40 HU predicts approximately 30% hepatic fat content, depending on the normalization method used.[13,14] Furthermore, SAT attenuation correlates with adipocyte size and lipid content, and the volume of pericardial adipose tissue (PAT), SAT, and VAT depots is associated with higher cardiovascular disease (CVD), diabetes, and NAFLD risk in HIV-negative persons.[15-18]

Although a link between lipoatrophic SAT and NAFLD was recognized early in the antiretroviral therapy (ART) era,[19] the specific changes in SAT gene expression accompanying hepatic steatosis among PWH on modern treatment regimens are not well understood. Furthermore, it is unclear whether hepatic steatosis, VAT expansion, cardiac and SM lipid deposition derive from similar changes in adipocyte gene expression, or whether each reflects unique perturbations. Relationships between ectopic depots are not well characterized, and it is not known whether hepatic lipid content is proportional

ARTICLE INFORMATION:

From the [1]Division of Gastroenterology, Hepatology and Nutrition, Vanderbilt University Medical Center, Nashville, TN, USA; [2]Tennessee Center for AIDS Research, Vanderbilt University Medical Center, Nashville, TN, USA; [3]Department of Biostatistics, Vanderbilt University Medical Center, Nashville, TN, USA; [4]Department of Radiology and Radiological Sciences, Vanderbilt University Medical Center, Nashville, TN, USA; [5]Veterans Affairs Tennessee Valley Healthcare System, Nashville, TN, USA; [6]Vanderbilt Technologies for Advanced Genomics, Vanderbilt University Medical Center, Nashville, TN, USA; [7]Division of Diabetes, Endocrinology and Metabolism, Vanderbilt University Medical Center, Nashville, TN, USA; [8]Division of Infectious Diseases, Vanderbilt University Medical Center, Nashville, TN, USA; [9]Division of Cardiovascular Medicine, Vanderbilt University Medical Center, Nashville, TN, USA.

ADDRESS CORRESPONDENCE AND REPRINT REQUESTS TO:

Curtis L. Gabriel, M.D., Ph.D.
Division of Gastroenterology, Hepatology and Nutrition
Vanderbilt University Medical Center
1030 MRBIV, 2215 Garland Ave.
Nashville, TN 37209
E-mail: curtis.L.gabriel@vumc.org
Tel.: +1-615-322-5200

to the volume and/or attenuation of other tissue compartments in PWH. We hypothesized that VAT volume and liver attenuation (as a marker of hepatic lipid infiltration) reflected a common profile of SAT dysfunction in PWH, which was not shared by other tissues prone to fat accumulation. To this end, we assessed the expression of multiple subcutaneous adipocyte regulatory and energy metabolism and storage genes in relation to ectopic lipid deposition in a cohort of PWH on long-term ART with sustained viral suppression.

Materials and Methods

STUDY POPULATION AND DESIGN

Adult PWH were recruited from the Vanderbilt Comprehensive Care Clinic between August 2017 and November 2019. Participants were on ART combination therapy for ≥18 months, with a minimum of 12 months of sustained suppression of plasma viremia at enrollment, and had no known inflammatory or rheumatologic conditions. Exclusion criteria were self-reported heavy alcohol use (>11 drinks/week), known cirrhosis, active hepatitis B or C, cocaine or amphetamine use, and use of corticosteroids or growth hormones. Participants provided written, informed consent, and the study was approved by the Vanderbilt University Institutional Review Board (ClinicalTrials. gov Identifier: NCT04451980).

ADIPOSE TISSUE BIOPSY

Abdominal adipose tissue biopsies were performed in the morning in the fasted state. SAT was collected about 3 cm to the right of the umbilicus using a 2.1-mm blunt side-ported liposuction catheter (Tulip CellFriendly GEMS Miller Harvester, Tulip Medical Products, San Diego, CA) after anesthetizing the skin with lidocaine and infiltrating 40 mL of sterile saline and lidocaine as tumescent fluid.[20] Tissue was aspirated into a 40-cc syringe, immediately placed in 40-50 cc of cold saline, and mixed to rinse. Visible blood vessels or clots were removed, and the sample was transferred to a 70-μm mesh filter for repeated saline rinses on ice with constant stirring. SAT was aliquoted into 1-mL vials and snap-frozen in liquid nitrogen.

RNA EXPRESSION ANALYSIS

Total RNA was extracted after mechanical lysis of the SAT aliquots with the Qiagen RNeasy Lipid Tissue Kit (Germantown, MD). mRNA expression levels were measured using an nCounter Plex (Nanostring, Seattle, WA) custom panel containing probes for 77 genes specific to adipocyte cellular regulation and lipid metabolism. mRNA expression was normalized to housekeeping genes and controlled with 14 synthetic spike-ins. The coefficient of variation (CV) of the positive controls is proportional to the technical variability introduced by the nCounter platform. The CV for the housekeeping controls is proportional to the confounding biological variation due to sample input. The mean endogenous CV shows the global noise of experimentally observed genes. We developed a normalization strategy based on CV values that includes the following steps. First, background count levels were calculated using the mean of negative controls and then subtracted from each sample. The normalization factor for sample/RNA content was then calculated using the geometric mean of a set of prespecified annotated housekeeping genes. The algorithm was normalized for sample or RNA content ("pipetting" fluctuations) using the geometric mean of prespecified annotated housekeeping genes. Finally, the count data were then divided by the normalization factor to generate counts normalized to the geometric mean of housekeeping genes.

CT IMAGING

All CT imaging was performed on a Siemens Somatom Force multidetector scanner (Erlangen, Germany). Separate noncontrast electrocardiogram-gated thorax (top of the aortic arch through the lung base) and abdominal (diaphragm to lumbosacral junction) scans were performed using a scanning protocol and image interpretation approach previously described.[21-23] Abdominal SAT and VAT volumes were measured within a 10-mm block of images consisting of eight images, 1.25-mm thick, at the L4-5 vertebrae[21,23] using Osirix software.

Total abdominal SM (psoas, quadratus lumborum, transversus abdominis, external and internal obliques, and rectus abdominis) mass and radiodensity were calculated at L4-L5 using an automated segmentation

software developed at the University of Alberta.[24] Tissue radiodensity was quantified using the HU scale, in which water has a value of 0 HU and air has a value of –1,000 HU. Shape modeling was used for SM analysis to segment out SAT at –190 HU to –30 HU and VAT at –150 HU to –50 HU. The muscle, SAT, and VAT regions were expanded to capture pixels near region borders. Final segmentation of each region was performed by taking only pixels in the valid HU range for each tissue. Images with abnormal muscle shapes were corrected manually by trained staff of the Vanderbilt Diet, Body Composition, and Human Metabolism Core.

Liver fat was analyzed using open-source OsiriX software custom-programmed subroutines.[25] Images at T12-L1 were used to identify the liver below the right diaphragm corresponding to superior aspects of the right and medial lobes or hepatic segments 4a, 7, and 8 using the Couinaud system. Three regions of interest were measured within homogenous portions of the liver on each of three different CT slices, and liver attenuation was averaged from the nine total regions.

PAT volume was measured within a 45-mm block of images spanning 15 mm above and 30 mm below the superior extent of the left main coronary artery, which includes the adipose tissue located around the epicardial coronary arteries (left main coronary, left anterior descending, right coronary, and circumflex arteries) as well as the epicardial and PAT around the coronary arteries, as previously described in detail.[25,26]

PLASMA LIPIDS

Fasting plasma high-density lipoprotein (HDL), low-density lipoprotein (LDL), and triglycerides were measured using the selective enzyme hydrolysis method (Abbott, Chicago, IL).

STATISTICS AND DATA VISUALIZATION

Spearman correlation coefficients (r_s) were calculated for tissue lipid depots and fasting plasma lipids using SPSS statistical software, and heatmaps were created using the "ComplexHeatmap" R package. All genes were assessed in a multivariable setting. Linear regression models were used to estimate the association between SAT gene expression to plasma lipid levels or tissue characteristics on CT. Models were adjusted for age, sex, race, BMI, diabetes status, CD4+ T-cell count at clinic enrollment or ART initiation, duration of ART, prior exposure to thymidine analogues (i.e., azidothymidine [AZT] or stavudine [d4T]), ART regimen class, and analysis batch. Gene-expression data were $\log_2$-transformed to improve normality before model fitting. False discovery rate (FDR)–adjusted P values were reported to account for multiple testing and were derived from the total 77 gene probes included in the assay, as opposed to the number of measured genes in specific pathways (as many pathways overlap).

A network diagram between gene expression and lipid variables, as well as CT scan variables, was created with Cytoscape software[27] to visualize the multidimensional interaction network. Genes with a nominal P value < 0.05 were included in the diagram to visualize the network. Nodes with smaller betweenness centrality have smaller sizes and brighter color. Edge size was based on statistical significance of the association between each CT/lipid variable and gene estimated in the linear regression models, adjusted for demographic variables, clinic variables, and batch effect. The edges are darker and larger for more significant results. A heatmap correlates gene expression with fasting lipids and CT characteristics of tissue lipid depots based on Spearman's correlations. Hierarchal clustering was used for row characteristics.

Results

COHORT CLINICAL DEMOGRAPHICS

Of the 97 participants, 75 (77%) were male and 52 (54%) were Caucasian (Table 1). The mean age was 47 years and mean BMI was 33.4 ± 6.3 kg/m². Female participants had higher BMI (P = 0.02), greater SAT volume (P < 0.005), lower SM attenuation (P < 0.005), and higher HDL levels (P = 0.004). There were no significant differences between males and females by age, CD4+ T-cell count, duration of ART, LDL-cholesterol, triglycerides, liver attenuation, VAT volume, VAT attenuation, PAT volume, or SAT attenuation.

TABLE 1. DEMOGRAPHIC CHARACTERISTICS OF PATIENT COHORT

	Female (n = 22)	Male (n = 75)	Combined (n = 97)
Demographics and clinical characteristics			
Age, years	46 ± 10	47 ± 12	47 ± 11
Race			
African American, % (n)	55% (12)	36% (27)	40% (39)
Caucasian, % (n)	36% (8)	59% (44)	54% (52)
Other, % (n)	9% (2)	5% (4)	6% (6)
BMI, (kg/m^2)	36.1* ± 8.7	32.6* ± 5.3	33.4 ± 6.3
CD4 count at start of ART or clinic enrollment, cells/mm^3	547 ± 362	476 ± 235	492 ± 269
Duration of ART, years	8.3 ± 5.1	9.0 ± 7.1	8.8 ± 6.7
Recorded exposure to AZT or d4T			
Yes (n)	23% (5)	13% (10)	15% (15)
No (n)	77% (17)	87% (65)	85% (82)
ART regimen at time of study enrollment			
NNRTI and NRTI	5% (1)	19% (14)	15% (15)
Integrase inhibitor and NRTI	64% (14)	55% (41)	57% (55)
Integrase inhibitor and protease inhibitor	5% (1)	4% (3)	4% (4)
Protease inhibitor and NRTI	14% (3)	11% (8)	11% (11)
Other	14% (3)	12% (9)	12% (12)
Diabetes status			
Insulin sensitive (n)	32% (7)	40% (30)	38% (37)
Prediabetic (n)	36% (8)	35% (26)	35% (34)
Diabetic (n)	32% (7)	25% (19)	27% (26)
Lipids and lipoproteins			
Fasting triglyceride, mg/dL	154.7 ± 96.3	180 ± 152.5	174.3 ± 141.6
Fasting HDL, mg/dL	54.8† ± 18.0	43.3† ± 15.5	45.9 ± 16.7
Fasting LDL, mg/dL	107.6 ± 25.6	101.6 ± 37.4	103.0 ± 35
Adipose tissue, muscle and liver volume, and attenuation			
Visceral fat volume, cm^3	155.1 ± 81.5	184.3 ± 98.3	177.9 ± 95.3
Pericardial fat volume, cm^3	73.6 ± 62.9	73.8 ± 49.2	73.7 ± 52.2
Subcutaneous fat volume, cm^3	491† ± 168	323† ± 124	360 ± 151
Subcutaneous fat attenuation, HU	−100.4 ± 5.5	−98.5 ± 6.6	−98.9 ± 6.4
SM attenuation, HU	33.2† ± 6.4	40.9† ± 5.4	39.2 ± 6.5
Visceral fat attenuation, HU	−97.8 ± 5.3	−97.6 ± 6.3	−97.7 ± 6.0
Liver attenuation, HU	61.6 ± 9.1	60.6 ± 9.9	60.8 ± 9.7

Note: Student t test was used to measure lab values and lipid depots of male and female participants. Diabetes status was defined as follows: insulin sensitive, HbA1c < 5.7 or FBG < 100 mg/dL; prediabetic, HbA1c 5.7%-6.4% and/or FBG 100-126 mg/dL, HbA1c ≥ 6.4%, and/or FBG ≥ 126 mg/dL and on diabetes medications.
*P < 0.05.
†P < 0.005.
Abbreviations: FBG, fasting blood glucose; HbA1c, hemoglobin A1c; NNRTI, non-nucleoside reverse transcriptase inhibitors; NRTI, nucleoside analog reverse-transcriptase inhibitors.

RELATIONSHIPS AMONG BMI, FASTING LIPIDS, ADIPOSE DEPOT VOLUMES, AND TISSUE ATTENUATION

Relationships among plasma lipids, adipose tissue depot size, and tissue density are shown in Fig. 1. Lower liver attenuation was associated with greater VAT volume (r_s = −0.48), PAT volume (r_s = −0.29), triglycerides (r_s = −0.35), and BMI (r_s = −0.40). Higher liver attenuation was associated with higher VAT attenuation (r_s = 0.434), and HDL level (r_s = 0.395). There were no significant associations between liver attenuation and SAT volume, SAT attenuation, or
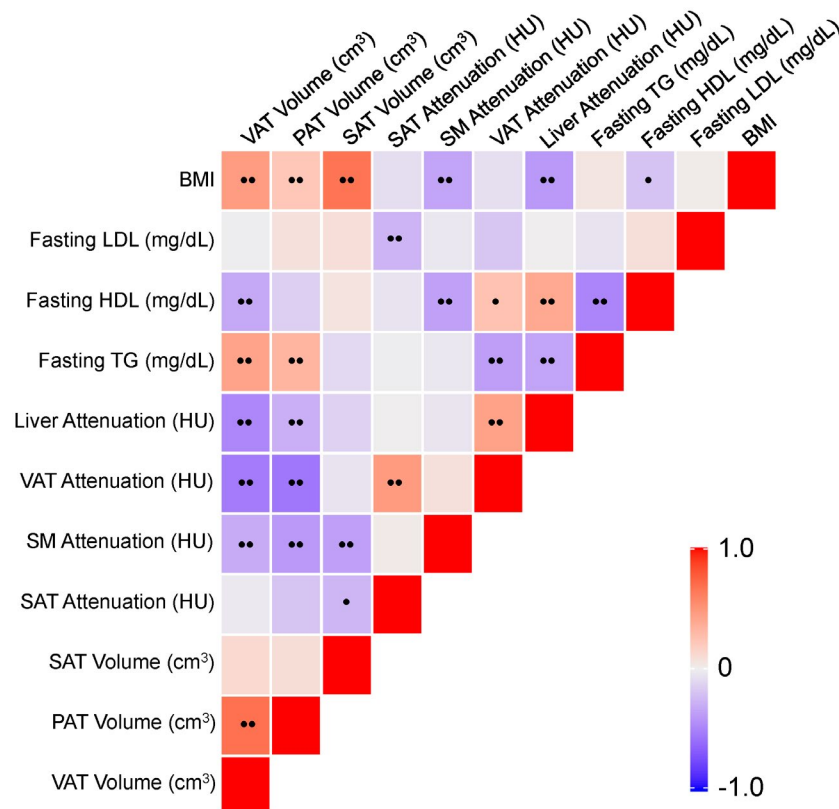
FIG. 1. Relationships among BMI, fasting lipids, and adipose tissue depot size and density. Spearman correlation coefficients between tissue density (HU), tissue volume, fasting plasma lipids, and BMI in 97 PWH. •P < 0.05, ••P < 0.01. Abbreviation: TG, triglyceride.

SM attenuation. However, VAT attenuation positively correlated with SAT attenuation (r_s = 0.472) and negatively correlated with VAT volume (r_s = –0.539). VAT volume was positively associated with PAT volume (r_s = 0.689) and triglycerides (r_s = 0.429).

SAT GENE-EXPRESSION PATTERNS RELATED TO ECTOPIC LIPID DEPOTS AND PLASMA LIPIDS

Relationships of SAT genes specific to adipocyte regulation and lipid metabolism with tissue lipid depots are shown in Fig. 2. Liver attenuation, VAT attenuation, and HDL were associated with similar SAT gene-expression profiles.

Genes with nominal P values of < 0.05 are ranked for tissues and plasma lipids in Tables 2 and 3, respectively. These tables also include FDR-adjusted P values based on the total of 77 gene probes included in the assay, rather than the number of measured genes

in specific pathways. There were significant associations, based on nominal P values, between SAT gene expression and SAT attenuation, VAT attenuation, VAT volume, liver attenuation, and plasma lipids. Lower liver attenuation was associated with higher expression of phospholipid transfer protein (*PLTP),* but lower expression of acyl-coenzyme A dehydrogenase medium (*ACADM*), adiponectin (*ADIPOQ*), and lipoprotein lipase (*LPL*). Lower VAT attenuation was also associated with lower expression of *ADIPOQ, LPL* and *ACADM,* and higher expression of leptin (*LEP*) and oxidized LDL receptor 1 (*OLR1*). Greater VAT volume was associated with higher SAT expression of *PLTP*, and lower *LPL* and peroxisome proliferator activated receptor delta (*PPARD*) expression.

Higher circulating triglycerides and lower HDL were both associated with lower SAT expression of *ACADM, ADIPOQ,* and fatty acid synthase (*FASN*) expression. Finally, higher LDL levels were associated
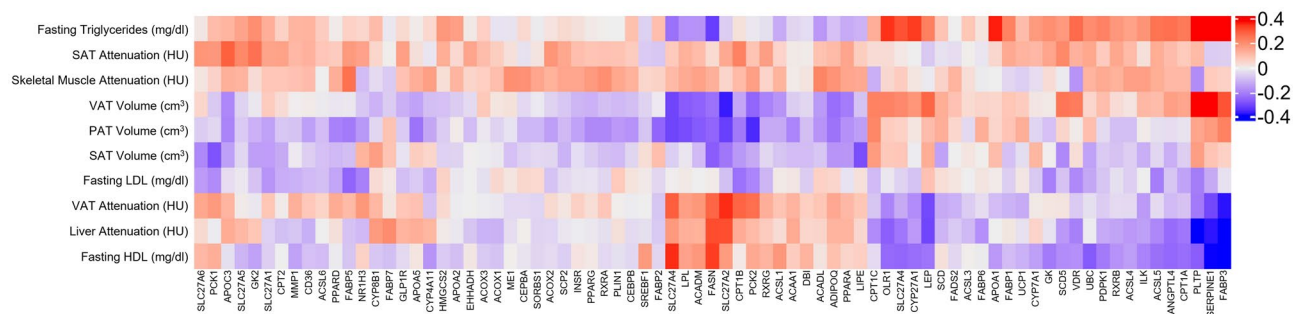
FIG. 2. Correlation of SAT gene expression with fasting lipids, adipose tissue depot size, or tissue density. Heatmap showing relationships between whole adipose tissue gene expression (columns) with fasting lipids and CT characteristics of tissue depots (rows) using adjusted Spearman correlations. Models were adjusted for age, sex, race, BMI, diabetes status, CD4 count at clinic enrollment, duration of ART, exposure to AZT or d4T antiviral therapy, and batch effect (see Supplementary Material).

with lower SAT expression of *PPARD*, insulin receptor, glucose transporter type 4 (*SLC2A4*), fatty acid binding protein 5 (*FABP5*), 3-phosphoinositide dependent protein kinase 1, and phosphoenolpyruvate carboxykinase 2.

LIVER ATTENUATION AND VISCERAL FAT ATTENUATION ARE CLOSELY RELATED ON NETWORK ANALYSIS

A network diagram of tissue compartments and plasma lipids, linked by genes with a nominal *P* value < 0.05, is shown in Fig. 3. Liver attenuation closely clustered with VAT attenuation, plasma triglycerides, and HDL based on shared expression of *FASN, ADIPOQ,* and *ACADM*; the positioning of SAT volume is principally due to shared *ADIPOQ* expression. There were no strong linkages among SAT attenuation, PAT volume, VAT volume, fasting LDL, or SM attenuation with liver attenuation or VAT attenuation.

Discussion

Over 1.1 million people in the United States are living with HIV,[28] and as these individuals survive decades on effective ART they are at higher risk of developing NAFLD and other metabolic diseases compared with the general population.[4-6] PWH with hepatic steatosis also develop steatohepatitis and hepatic fibrosis at higher rates than HIV-negative

persons with NAFLD,[5,6] which further increases morbidity and mortality through the complications of cirrhosis and hepatocellular carcinoma. In this study, we used CT imaging to quantify the volume and attenuation of adipose tissue and attenuation of SM and liver in a cohort of PWH with long-term plasma viral suppression on modern ART regimens. These CT-derived characteristics were associated with differences in SAT adipose gene expression. Impaired adipose tissue energy storage and regulation plays a key role in the pathogenesis of the metabolic syndrome and NAFLD in HIV-negative persons,[29] and this effect can be potentiated in PWH[30] due to HIV and ART-related changes in adipose tissue distribution, cellular composition, and adipocyte function. PWH are prone to developing lipodystrophy characterized by lipoatrophy of SAT and lipohypertrophy of VAT,[31] and there is emerging evidence that adipose tissue attenuation in different depots can provide information on adipocyte size and adipose tissue structure—features that are associated with the risk of cardiovascular comorbidities. Specifically, Lee et al. showed that VAT and SAT attenuation had differing relationships with circulating markers of CVD risk in HIV-negative persons.[32,33]

SAT is an important HIV reservoir, and latently infected CD4⁺ T cells and macrophages release viral proteins that decrease adipocyte expression of major transcription factors critical to cellular function, such as peroxisome proliferator-activated receptor γ (*PPARG*).[34] Alteration in critical transcription factors results in reduced expression of lipid storage genes,

TABLE 2. SIGNIFICANT SAT GENES ASSOCIATED WITH ECTOPIC LIPID DEPOT SIZE AND DENSITY

	Gene Name or Alias	Function	P Value	p$_{adj}$ Value	Estimate
Visceral fat volume					
PLTP	Phospholipid transfer protein	Lipid transport	<0.001	0.013	0.0053
LPL	Lipoprotein lipase	Triglyceride metabolism	0.006	0.17	−0.0028
HMGCS2	3-hydroxy-3-methylglutaryl-CoA synthase 2	Cholesterol synthesis and ketogenesis	0.006	0.17	−0.0211
ACSL6	Acyl-CoA synthetase long-chain family member 6	Fatty acid synthesis	0.001	0.19	−0.0117
APOC3	Apolipoprotein C3	Triglyceride metabolism	0.02	0.24	−0.0156
FABP7	Fatty acid binding protein 7	Fatty acid transport	0.02	0.24	−0.0173
SCD5	Stearoyl-CoA desaturase 5	Fatty acid metabolism	0.04	0.35	0.0097
SCL27A5	Solute carrier family 27 member 5	Bile acid metabolism and fatty acid synthesis	0.04	0.35	−0.0173
PPARD	Peroxisome proliferator activated receptor delta	Fatty acid metabolism	0.04	0.35	0.0142
PLIN1	Perilipin 1	Adipocyte lipid metabolism	0.049	0.35	−0.0018
Pericardial fat volume					
SERPINE1	Serpin family E member 1	Plasminogen activator	0.001	0.33	0.0285
CPT1C	Carnitine palmitoyltransferase 1C	Fatty acid oxidation	0.01	0.33	0.0322
OLR1	Oxidized low-density lipoprotein receptor 1	Lipid metabolism	0.02	0.33	0.035
ME1	Malic enzyme 1	Fatty acid synthesis	0.02	0.33	0.0267
FABP6	Fatty acid binding protein 6	Fatty acid transport	0.03	0.39	0.0216
SLC27A4	Solute carrier family 27 member 4	Fatty acid transport	0.04	0.39	0.0236
MMP1	Matrix metallopeptidase 1	Collagen cleavage	0.04	0.39	−0.0253
RXRB	Retinoid X receptor beta	Retinoic acid, thyroid hormone and vitamin D signaling	0.04	0.39	0.0224
ACSL4	Acyl-CoA synthetase long chain family member 4	Fatty acid metabolism	0.046	0.39	0.0225
Subcutaneous fat volume					
CYP8B1	Cytochrome P450 family 8 subfamily B member 1	Lipid synthesis	0.006	0.31	0.0128
ACAA1	Acetyl-CoA acyltransferase 1	Fatty acid oxidation	0.008	0.31	−0.002
CPT1C	Carnitine palmitoyltransferase 1C	Lipid metabolism	0.02	0.31	0.0130
DBI	Diazepam binding inhibitor, acyl-CoA binding protein	Lipid metabolism	0.02	0.31	−0.0022
CYP4A11	Cytochrome P450 family 4 subfamily A member 11	Fatty acid metabolism	0.02	0.31	0.0141
FABP7	Fatty acid binding protein 7	Fatty acid transport	0.03	0.31	0.0113
ADIPOQ	Adiponectin, C1Q, and collagen domain containing	Energy homeostasis	0.04	0.31	−0.0011
LEP	Leptin	Energy homeostasis	0.04	0.31	0.002
FABP2	Fatty acid binding protein 2	Fatty acid transport	0.04	0.31	0.0122
FABP1	Fatty acid binding protein 1	Fatty acid transport	0.04	0.31	0.0083
SCD5	Stearoyl-CoA desaturase 5	Fatty acid metabolism	0.04	0.31	−0.0065
Subcutaneous fat attenuation					
LEP	Leptin	Energy balance	<0.001	0.03	−0.0488
OLR1	Oxidized low-density lipoprotein receptor 1	Lipid metabolism	0.004	0.14	−0.2612
GK2	Glycerol kinase 2	Glycerol synthesis	0.01	0.26	0.2137
SLC27A5	Solute carrier family 27 member 5	Bile acid metabolism and fatty acid synthesis	0.04	0.63	0.1877
GLP1R	Glucagon like peptide 1 receptor	Insulin secretion, adipose tissue metabolism	0.04	0.63	0.1775

TABLE 2. *Continued*

Gene Name or Alias		Function	P Value	p$_{adj}$ Value	Estimate
SM attenuation					
SCD	Stearoyl-CoA desaturase	Fatty acid synthesis	0.02	0.45	−0.1625
SLC27A6	Fatty acid transport protein 6	Fatty acid transport	0.03	0.45	−0.2276
RXRB	Retinoid X receptor beta	Retinoic acid, thyroid hormone and vitamin D signaling	0.03	0.45	−0.230
SLC27A2	Very long-chain acyl-CoA synthetase	Fatty acid synthesis	0.04	0.45	−0.2984
FABP1	Fatty acid binding protein 1	Fatty acid transport	0.049	0.45	−0.1876
Visceral fat attenuation					
LEP	Leptin	Energy homeostasis	<0.001	<0.001	−0.0703
ADIPOQ	adiponectin, c1q, and collagen domain containing	Energy homeostasis	<0.001	0.005	0.0321
OLR1	oxidized low density lipoprotein receptor 1	Lipid metabolism	0.001	0.04	−0.3198
ACADM	Acyl-CoA dehydrogenase medium chain	Fatty acid oxidation	0.002	0.04	0.0272
FASN	Fatty acid synthase	Fatty acid synthesis	0.009	0.12	0.0626
SLC27A2	Very long-chain acyl-CoA synthetase	Fatty acid synthesis	0.009	0.12	0.280
FABP5	Fatty acid binding protein 5	Fatty acid transport	0.01	0.14	0.0246
LPL	Lipoprotein lipase	Triglyceride metabolism	0.02	0.15	0.0295
PLTP	Phospholipid transfer protein	Lipid transport	0.02	0.19	−0.039
APOC3	Apolipoprotein C3	Triglyceride metabolism	0.04	0.30	0.159
Liver attenuation					
PLTP	Phospholipid transfer protein	Lipid transport	<0.001	0.008	−0.0388
ACADM	Acyl-CoA dehydrogenase medium chain	Fatty acid oxidation	0.001	0.02	0.0178
LPL	Lipoprotein lipase	Triglyceride metabolism	0.001	0.02	0.0247
APOC3	Apolipoprotein C3	Triglyceride metabolism	0.005	0.09	0.130
ADIPOQ	Adiponectin, C1Q, and collagen domain containing	Energy homeostasis	0.009	0.10	0.0137
FABP7	Fatty acid binding protein 7	Fatty acid transport	0.009	0.10	0.137
FASN	Fatty acid synthase	Fatty acid synthesis	0.009	0.10	0.0377
SLC27A5	Solute carrier family 27 member 5	Bile acid metabolism and fatty acid synthesis	0.01	0.13	0.149
CYP7A1	Cytochrome P450 family 7 subfamily A member 1	Lipid synthesis	0.03	0.21	0.118
PLIN1	Perilipin 1	Adipocyte lipid metabolism	0.03	0.21	0.0147
ACSL1	Acyl-CoA synthetase long chain family member 1	Fatty acid oxidation	0.03	0.24	0.0183
UBC	Ubiquitin C	Cellular homeostasis	0.04	0.27	0.0917
FABP1	Fatty acid binding protein 1	Fatty acid transport	0.048	0.28	0.085

Note: Genes with nominal *P* value < 0.05 were included in the table. Gene name and general function are listed. Models were adjusted for age, sex, race, BMI, diabetes status, CD4+ T-cell count at clinic enrollment or ART initiation, duration of ART, prior exposure to thymidine analogue (i.e., AZT or d4T), ART regimen class, and assay batch. FDR-adjusted *P* values are based on the total 77 gene probes included in the assay rather than the number of measured genes in specific pathways.

reduced expression of adipokines important for insulin sensitization, and other endocrine functions, and increased expression of pro-inflammatory cytokines.[35] HIV proteins also promote increased production of extracellular matrix components (e.g., collagen I, VI, and fibronectin) by adipocytes and their precursors.[36]

Exposure to antiretroviral agents further impairs subcutaneous adipocyte function. Although many studies are from the era of prevalent ART-induced peripheral lipoatrophy,[37,38] a more recent study of modern agents found varying degrees of toxicity, even in those without clinically apparent lipoatrophy.[39] Major features of lipoatrophic SAT are decreased expression of transcription factors *PPARG*, CCAAT-enhancer-binding protein-α, sterol regulatory element-binding protein-1, and target genes regulating fatty

TABLE 3. SIGNIFICANT SAT GENES ASSOCIATED WITH FASTING PLASMA LIPIDS

	Gene Name or Alias	Function	P Value	p$_{adj}$ Value	Estimate
Fasting triglycerides					
ACSL1	Acyl-CoA synthetase long chain family member 1	Fatty acid oxidation	0.002	0.14	−0.002
LPL	Lipoprotein lipase	Triglyceride metabolism	0.01	0.40	−0.0014
FASN	Fatty acid synthase	Fatty acid synthesis	0.02	0.40	−0.0025
ACADM	Acyl-CoA dehydrogenase medium chain	Fatty acid oxidation	0.02	0.40	−0.0009
ADIPOQ	Adiponectin, C1Q, and collagen domain containing	Energy homeostasis	0.04	0.58	−0.0008
Fasting HDL					
ACADM	Acyl-CoA dehydrogenase medium chain	Fatty acid oxidation	<0.001	0.003	0.0127
ACSL1	Acyl-CoA synthetase long chain family member 1	Fatty acid oxidation	<0.001	0.01	0.0176
FASN	Fatty acid synthase	Fatty acid synthesis	<0.001	0.01	0.0295
ADIPOQ	adiponectin, C1Q, and collagen domain containing	Energy Homeostasis	0.002	0.04	0.0096
SLC2A4	Glucose transporter type 4	Glucose transport	0.007	0.10	0.0534
SLC27A6	Fatty acid transport protein 6	Fatty acid transport	0.008	0.10	0.0751
SLC27A2	Very long-chain acyl-CoA synthetase	Fatty acid synthesis	0.046	0.51	0.0776
Fasting LDL					
PDPK1	3-phosphoinositide dependent protein kinase 1	Energy homeostasis	<0.001	<0.001	−0.0275
INSR	Insulin receptor	Insulin signaling	<0.001	0.001	−0.026
SLC2A4	Glucose transporter type 4	Glucose transport	<0.001	0.002	−0.0342
FABP5	Fatty acid binding protein 5	Fatty acid transport	0.001	0.03	−0.0049
PCK2	Phosphoenolpyruvate carboxykinase 2, mitochondrial	Glucose metabolism	0.003	0.049	−0.0307
RXRG	Retinoid X receptor gamma	Retinoic acid signaling	0.004	0.05	−0.037
NR1H3	Nuclear receptor subfamily 1 group H member 3	Retinoic acid signaling	0.006	0.06	−0.0243
PLIN1	Perilipin 1	Adipocyte lipid metabolism	0.006	0.06	0.00480
ACSL3	Acyl-CoA synthetase long chain family member 3	Fatty acid synthesis	0.02	0.14	−0.0289
CPT1B	Carnitine palmitoyltransferase 1B	Fatty acid oxidation	0.02	0.16	−0.0317
PPARD	Peroxisome proliferator activated receptor delta	Fatty acid metabolism	0.04	0.29	−0.0273
SLC27A4	Solute carrier family 27 member 4	Fatty acid transport	0.046	0.29	−0.0265

Note: Genes with nominal P value < 0.05 were included in this table. Gene name and general gene function are listed. Models were adjusted for age, sex, race, BMI, diabetes status, CD4$^+$ T-cell count at clinic enrollment or ART initiation, duration of ART, prior exposure to thymidine analogue (i.e., AZT or d4T), ART regimen class and assay batch. FDR-adjusted P values are based on the total 77 gene probes included in the assay rather than the number of measured genes in specific pathways.

acid and glucose metabolism (e.g., *LPL,* glucose transporter type 4).[40] More recently, SAT and VAT from PWH on integrase strand transfer inhibitor–based ART were found to have greater tissue fibrosis compared with persons on non-nucleoside reverse transcriptase-based ART.[39]

Although most studies in HIV-negative persons rely on adipose tissue volume or area, attenuation may be a better indicator of tissue quality and function in people with clinically apparent or subclinical lipodystrophy, including PWH. Lower SAT attenuation was shown to be reflective of increased adipocyte size in PWH,[41] and lower attenuation was associated with prior exposure to ART regimens containing thymidine analogues.[42] The clinical significance of adipose tissue density in PWH has not been clearly defined, but may reflect fibrosis or local inflammation. Lake et al. showed that greater SAT and VAT attenuation was associated with higher levels of circulating inflammatory cytokines, independent of tissue area.[43] Conversely, another group showed that lower SAT and VAT attenuation was associated with higher levels of plasma inflammatory cytokines.[44] Unfortunately, our Nanostring panel did not include markers of inflammation, and we are unable to relate indices of VAT and SAT density to tissue inflammation.

CT imaging has previously been used to delineate relationships between VAT and SAT attenuation and volume with the risk of CVD, hypertension, diabetes, and NAFLD in HIV-negative persons.[15-18] However, there are limited data relating adipose tissue characteristics and metabolic disease in PWH, and to
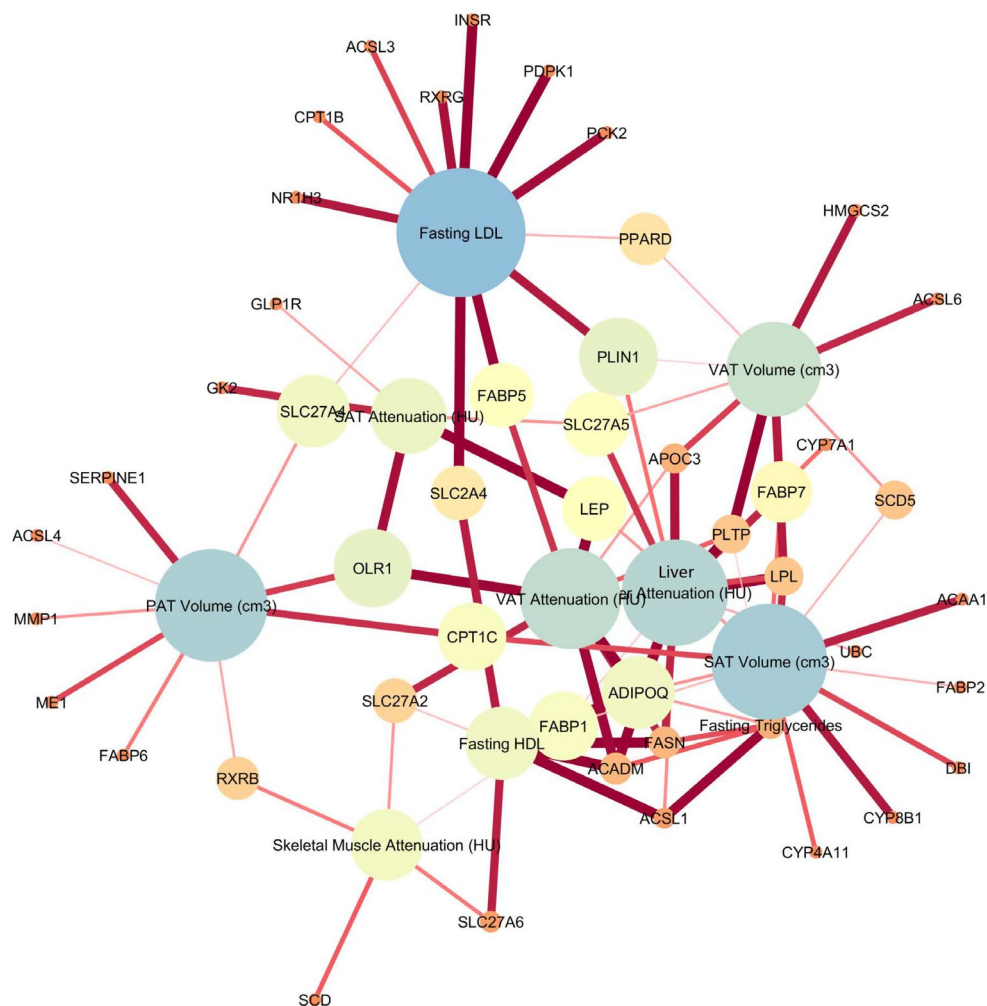
FIG. 3. Network analysis of gene–tissue relationships. All relationships between gene expression and tissue depots with raw *P* value < 0.05 are shown. Larger node size represents a greater degree of connectivity with other nodes. Connecting lines are darker and wider for smaller raw *P* values between expression of individual genes and plasma lipid levels or tissue characteristics on CT variables and gene expression (see Supplementary Material).

our knowledge, none that relate these characteristics to adipose gene expression. We found that lower liver attenuation (a surrogate marker of higher hepatic steatosis) was most closely correlated with greater VAT volume and lower VAT attenuation in our cohort of PWH on long-term ART. However, there was no significant relationship between liver attenuation and SAT attenuation or volume. Although SAT characteristics derived from CT did not correlate with liver attenuation, we identified a specific SAT geneexpression profile that was associated with a greater degree of hepatic steatosis, as measured by liver attenuation. Increased expression of *LPL* and *ACADM* was associated with higher liver attenuation (less steatosis)

after FDR adjustment, whereas *PLTP* expression was inversely associated with liver attenuation. Higher *FASN* and *ADIPOQ* expression were also associated with higher liver attenuation, but not after FDR adjustment. However, it should be noted that the FDR-adjusted *P* values were derived using the total 77 gene probes included in the assay, as opposed to the number of measured genes in specific pathways (given that many of the pathways overlap).

Adiponectin suppresses adipocyte lipolysis and stimulates hepatic fatty acid oxidation, which promotes lipid homeostasis through lipid storage in the adipocyte and fatty acid disposal in the liver.[45] Gelpi et al. showed that higher plasma adiponectin levels

in PWH were associated with higher VAT density—independent of VAT area. Reduced levels of *LPL*, an enzyme necessary for cellular lipid uptake of fatty acids from the bloodstream, is associated with hypertriglyceridemia, obesity, and metabolic syndrome.[46] *FASN*, a key component of the *de novo* lipogenesis pathway, further promotes the storage of lipids in adipose tissue.[47] We hypothesize that this gene-expression profile contributes to a lipid "spillover" from the SAT to the liver, in which triglyceride storage in SAT is impaired through lower activity of *LPL* and increased lipolysis. Overall, these results emphasize the role of SAT function in the pathogenesis of NAFLD in PWH.

Our analysis highlighted several genes that have previously been associated with metabolic disease or lipodystrophy in PWH. Polymorphisms in *LPL* were shown to be protective against dyslipidemia in PWH,[48] whereas HDL-associated *PLTP* protein levels were shown to be positively correlated with viral load and negatively correlated with CD4+ T-cell counts in PWH.[49] Finally, HIV infection was previously shown to increase *FASN* levels in cell culture[50]; however, the relationship between adipose *FASN* and hepatic steatosis has not previously been explored in PWH.

Our study has several limitations. Liver attenuation, as measured by HU on CT imaging, was used as a surrogate marker of hepatic steatosis and SM lipid content. Although this approach is used in several studies, other methodologies including biopsy and magnetic resonance imaging–proton density fat fraction may provide better estimates of lipid content compared with CT imaging. Furthermore, we do not have direct measures of steatohepatitis or fibrosis. Inclusion of NAFLD staging in future analyses may reveal other unique associations that were not apparent with our focus on liver attenuation. Our Nanostring panel probed a prespecified set of adipocyte-related genes, which limited our analysis to these targets. Specifically, the panel did not include genes related to SAT inflammation or fibrosis. Future studies in our cohort will use next-generation sequencing to obtain an unbiased landscape of the adipose tissue transcriptome. The mean BMI of the cohort was 33.4, and although BMI was included as a covariate in our analysis, the number of participants with class 2 and class 3 obesity may limit the generalizability of our study. Finally, this was a cross-sectional analysis of prevalent hepatic steatosis that focused on PWH. Therefore, we do not know whether these results are generalizable to HIV-negative persons, and we cannot define a temporal relationship between changes in SAT gene expression and the development of hepatic steatosis. Future studies will include HIV-negative persons as well as an additional imaging time point that will allow us to overcome this limitation. We used a stringent FDR-adjusted significance cutoff in our analysis based on the total number of gene probes in the assay, which may have underestimated the strength of relationships between gene expression and ectopic lipid measures. Additional studies are needed for confirmation of our results and to determine the biological relevance of genes that did not reach FDR-adjusted significance.

In conclusion, we show that changes in expression of SAT lipid homeostasis genes, including *ACADM*, *LPL* and *PLTP*, were associated with increased hepatic steatosis. The pattern of SAT gene expression associated with higher levels of hepatic steatosis was similar in those with lower fasting HDL and decreased visceral fat attenuation, but not with PAT attenuation or SM attenuation. Decreased VAT attenuation and increased VAT volume on CT scan were associated with decreased liver attenuation, but we did not find a significant association between liver attenuation and SAT attenuation or volume. This indicates that the relationships between SAT function and ectopic fat deposition are not uniform across lipid depots. Future studies will evaluate relationships between the plasma lipidome and NAFLD in PWH and HIV-negative persons, and will determine whether strategies to improve adipose tissue health (e.g., changes in ART therapy, pharmacotherapy, or management of metabolic comorbidities) can improve liver-related outcomes in this population disproportionately affected by NAFLD.

REFERENCES

1) Weber R, Sabin CA, Friis-Møller N, Reiss P, El-Sadr WM, Kirk O, et al. Liver-related deaths in persons infected with the human immunodeficiency virus: the D:A: D study. Arch Intern Med 2006;166:1632-1641.

2) Nansseu JR, Bigna JJ, Kaze AD, Noubiap JJ. Incidence and risk factors for prediabetes and diabetes mellitus among HIV-infected adults on antiretroviral therapy: a systematic review and meta-analysis. Epidemiology 2018;29:431-441.

3) Currier JS, Lundgren JD, Carr A, Klein D, Sabin CA, Sax PE, et al. Epidemiological evidence for cardiovascular disease in

HIV-infected patients and relationship to highly active antiretroviral therapy. Circulation 2008;118:e29-e35.

4) Maurice JB, Patel A, Scott AJ, Patel K, Thursz M, Lemoine M. Prevalence and risk factors of nonalcoholic fatty liver disease in HIV-monoinfection. AIDS 2017;31:1621-1632.

5) Lui G, Wong VW-S, Wong Gl-H, Chu WC-W, Wong C-K, Yung IMH, et al. Liver fibrosis and fatty liver in Asian HIV-infected patients. Aliment Pharmacol Ther 2016;44:411-421.

6) Vodkin I, Valasek MA, Bettencourt R, Cachay E, Loomba R. Clinical, biochemical and histological differences between HIV-associated NAFLD and primary NAFLD: a case-control study. Aliment Pharmacol Ther 2015;41:368-378.

7) Younossi ZM, Koenig AB, Abdelatif D, Fazel Y, Henry L, Wymer M. Global epidemiology of nonalcoholic fatty liver disease—meta-analytic assessment of prevalence, incidence, and outcomes. Hepatology 2016;64:73-84.

8) Mohammed SS, Aghdassi E, Salit IE, Avand G, Sherman M, Guindi M, et al. HIV-positive patients with nonalcoholic fatty liver disease have a lower body mass index and are more physically active than HIV-negative patients. J Acquir Immune Defic Syndr 2007;45:432-438.

9) Kusminski CM, Bickel PE, Scherer PE. Targeting adipose tissue in the treatment of obesity-associated diabetes. Nat Rev Drug Discov 2016;15:639-660.

10) McComsey GA, Kitch D, Sax PE, Tebas P, Tierney C, Jahed NC, et al. Peripheral and central fat changes in subjects randomized to abacavir-lamivudine or tenofovir-emtricitabine with atazanavir-ritonavir or efavirenz: ACTG Study A5224s. Clin Infect Dis 2011;53:185-196.

11) Koethe JR, Lagathu C, Lake JE, Domingo P, Calmy A, Falutz J, et al. HIV and antiretroviral therapy-related fat alterations. Nat Rev Dis Primers 2020;6:48.

12) Gallego-Escuredo JM, Villarroya J, Domingo P, Targarona EM, Alegre M, Domingo JC, et al. Differentially altered molecular signature of visceral adipose tissue in HIV-1-associated lipodystrophy. J Acquir Immune Defic Syndr 2013;64:142-148.

13) Goodpaster BH, Kelley DE, Thaete FL, He J, Ross R. Skeletal muscle attenuation determined by computed tomography is associated with skeletal muscle lipid content. J Appl Physiol 1985;2000:104-110.

14) Kodama Y, Ng CS, Wu TT, Ayers GD, Curley SA, Abdalla EK, et al. Comparison of CT methods for determining the fat content of the liver. AJR Am J Roentgenol 2007;188:1307-1312.

15) Kim D, Chung GE, Kwak M-S, Seo HB, Kang JH, Kim W, et al. Body fat distribution and risk of incident and regressed nonalcoholic fatty liver disease. Clin Gastroenterol Hepatol 2016;14:e134.

16) Chung GE, Kim D, Kwark MS, Kim W, Yim JY, Kim YJ, et al. Visceral adipose tissue area as an independent risk factor for elevated liver enzyme in nonalcoholic fatty liver disease. Medicine (Baltimore) 2015;94:e573.

17) Côté JA, Nazare JA, Nadeau M, Leboeuf M, Blackburn L, Després JP, et al. Computed tomography-measured adipose tissue attenuation and area both predict adipocyte size and cardiometabolic risk in women. Adipocyte 2016;5:35-42.

18) Verboven K, Wouters K, Gaens K, Hansen D, Bijnen M, Wetzels S, et al. Abdominal subcutaneous and visceral adipocyte size, lipolysis and inflammation relate to insulin resistance in male obese humans. Sci Rep 2018;8:4677.

19) Polyzos SA, Perakakis N, Mantzoros CS. Fatty liver in lipodystrophy: a review with a focus on therapeutic perspectives of adiponectin and/or leptin replacement. Metabolism 2019;96:66-82.

20) Alexander RW, Harrell DB. Autologous fat grafting: use of closed syringe microcannula system for enhanced autologous structural grafting. Clin Cosmet Investig Dermatol 2013;6:91-102.

21) VanWagner LB, Ning H, Lewis CE, Shay CM, Wilkins J, Carr JJ, et al. Associations between nonalcoholic fatty liver disease and subclinical atherosclerosis in middle-aged adults: the Coronary Artery Risk Development in Young Adults Study. Atherosclerosis 2014;235:599-605.

22) Carr JJ, Nelson JC, Wong ND, McNitt-Gray M, Arad Y, Jacobs DR, et al. Calcified coronary artery plaque measurement with cardiac CT in population-based studies: standardized protocol of Multi-Ethnic Study of Atherosclerosis (MESA) and Coronary Artery Risk Development in Young Adults (CARDIA) study. Radiology 2005;234:35-43.

23) Terry JG, Shay CM, Schreiner PJ, Jacobs DR, Sanchez OA, Reis JP, et al. Intermuscular adipose tissue and subclinical coronary artery calcification in midlife: the CARDIA Study (Coronary Artery Risk Development in Young Adults). Arterioscler Thromb Vasc Biol 2017;37:2370-2378.

24) Chung H, Cobzas D, Lieffers JR, Birdsell L, Baracos V. Automated segmentation of muscle and adipose tissue on CT images for human body composition analysis. In: Proceedings of the International Society for Optical Engineering 7261, San Diego, California; 2009:197-204.

25) Miljkovic I, Kuipers AL, Cvejkus RK, Carr JJ, Terry JG, Thyagarajan B, et al. Hepatic and skeletal muscle adiposity are associated with diabetes independent of visceral adiposity in nonobese African-Caribbean men. Metab Syndr Relat Disord 2020;18:275-283.

26) Alman AC, Jacobs DR, Lewis CE, Snell-Bergeon JK, Carnethon MR, Terry JG, et al. Higher pericardial adiposity is associated with prevalent diabetes: the Coronary Artery Risk Development in Young Adults study. Nutr Metab Cardiovasc Dis 2016;26:326-332.

27) Shannon P, Markiel A, Ozier O, Baliga NS, Wang JT, Ramage D, et al. Cytoscape: a software environment for integrated models of biomolecular interaction networks. Genome Res 2003;13:2498-2504.

28) National Center for HIV/AIDS, Viral Hepatitis, STD, and TB Prevention Division of HIV/AIDS Prevention. Estimated HIV incidence and prevalence in the United States, 2010-2016. In: HIV Surveillance Supplemental Report 2019, Volume 24.

29) Rasouli N, Molavi B, Elbein SC, Kern PA. Ectopic fat accumulation and metabolic syndrome. Diabetes Obes Metab 2007;9:1-10.

30) Bailin SS, Gabriel CL, Wanjalla CN, Koethe JR. Obesity and weight gain in persons with HIV. Curr HIV/AIDS Rep 2020;17:138-150.

31) Bacchetti P, Gripshover B, Grunfeld C, Heymsfield S, McCreath H, Osmond D, et al. Fat distribution in men with HIV infection. J Acquir Immune Defic Syndr 2005;40:121-131.

32) Lee JJ, Pedley A, Hoffmann U, Massaro JM, Fox CS. Association of changes in abdominal fat quantity and quality with incident cardiovascular disease risk factors. J Am Coll Cardiol 2016;68:1509-1521.

33) Lee JJ, Britton KA, Pedley A, Massaro JM, Speliotes EK, Murabito JM, et al. Adipose tissue depots and their cross-sectional associations with circulating biomarkers of metabolic regulation. J Am Heart Assoc 2016;5:e002936.

34) Couturier J, Agarwal N, Nehete PN, Baze WB, Barry MA, Jagannadha Sastry K, et al. Infectious SIV resides in adipose tissue and induces metabolic defects in chronically infected rhesus macaques. Retrovirology 2016;13:30.

35) Giralt M, Domingo P, Guallar JP, Rodriguez de la Concepcion ML, Alegre M, Domingo JC, et al. HIV-1 infection alters gene expression in adipose tissue, which contributes to HIV-1/HAART-associated lipodystrophy. Antivir Ther 2006;11:729-740.

36) Gorwood J, Bourgeois C, Mantecon M, Atlan M, Pourcher V, Pourcher G, et al. Impact of HIV/simian immunodeficiency virus infection and viral proteins on adipose tissue fibrosis and adipogenesis. AIDS 2019;33:953-964.

37) Caron M, Auclair M, Lagathu C, Lombes A, Walker UA, Kornprobst M, et al. The HIV-1 nucleoside reverse transcriptase inhibitors stavudine and zidovudine alter adipocyte functions in vitro. AIDS 2004;18:2127-2136.

38) Rudich A, Ben-Romano R, Etzion S, Bashan N. Cellular mechanisms of insulin resistance, lipodystrophy and atherosclerosis induced by HIV protease inhibitors. Acta Physiol Scand 2005;183:75-88.

39) Gorwood J, Bourgeois C, Pourcher V, Pourcher G, Charlotte F, Mantecon M, et al. The integrase inhibitors dolutegravir and raltegravir exert pro-adipogenic and profibrotic effects and induce insulin resistance in human/simian adipose tissue and human adipocytes. Clin Infect Dis 2020 Mar 13. https://doi.org/10.1093/cid/ciaa259. [Epub ahead of print]

40) Bastard J-P, Caron M, Vidal H, Jan V, Auclair M, Vigouroux C, et al. Association between altered expression of adipogenic factor SREBP1 in lipoatrophic adipose tissue from HIV-1-infected patients and abnormal adipocyte differentiation and insulin resistance. Lancet 2002;359:1026-1031.

41) **Lake JE**, **Moser C**, Johnston L, Magyar C, Nelson SD, Erlandson KM, et al. CT fat density accurately reflects histologic fat quality in adults with HIV on and off antiretroviral therapy. J Clin Endocrinol Metab 2019;104:4857-4864.

42) Gelpi M, Knudsen AD, Larsen KB, Mocroft A, Lebech A-M, Lindegaard B, et al. Long-lasting alterations in adipose tissue density and adiponectin production in people living with HIV after thymidine analogues exposure. BMC Infect Dis 2019;19:708.

43) **Lake JE**, **Debroy P**, Ng D, Erlandson KM, Kingsley LA, Palella FJ, et al. Associations between subcutaneous fat density and systemic inflammation differ by HIV serostatus and are independent of fat quantity. Eur J Endocrinol 2019;181:451-459.

44) **Debroy P**, **Lake JE**, Moser C, Olefsky M, Erlandson KM, Scherzinger A, et al. Antiretroviral therapy initiation is associated with decreased visceral and subcutaneous adipose tissue density in people living with HIV. Clin Infect Dis 2020 Feb 28. https://doi.org/10.1093/cid/ciaa196. [Epub ahead of print]

45) Stern JH, Rutkowski JM, Scherer PE. Adiponectin, leptin, and fatty acids in the maintenance of metabolic homeostasis through adipose tissue crosstalk. Cell Metab 2016;23:770-784.

46) Mead JR, Irvine SA, Ramji DP. Lipoprotein lipase: structure, function, regulation, and role in disease. J Mol Med (Berl) 2002;80:753-769.

47) Song Z, Xiaoli AM, Yang F. Regulation and metabolic significance of *de novo* lipogenesis in adipose tissues. Nutrients 2018;10:1383.

48) Guardiola M, Echeverria P, González M, Vallvé JC, Puig J, Clotet B, et al. Polymorphisms in LPL, CETP, and HL protect HIV-infected patients from atherogenic dyslipidemia in an allele-dose-dependent manner. AIDS Res Hum Retroviruses 2015;31:882-888.

49) Rose H, Hoy J, Woolley I, Tchoua U, Bukrinsky M, Dart A, et al. HIV infection and high density lipoprotein metabolism. Atherosclerosis 2008;199:79-86.

50) Kulkarni MM, Ratcliff AN, Bhat M, Alwarawrah Y, Hughes P, Arcos J, et al. Cellular fatty acid synthase is required for late stages of HIV-1 replication. Retrovirology 2017;14:45.

Author names in bold designate shared co-first authorship.

Supporting Information

Additional Supporting Information may be found at onlinelibrary.wiley.com/doi/10.1002/hep4.1695/suppinfo.